Scanning Microscopy

Volume 1990
Number 4 *Fundamental Electron and Ion Beam Interactions with Solids for Microscopy, Microanalysis, and Microlithography*

Article 2

1990

Spatially Sensitive Electron Energy Loss Spectroscopy

Helmut Kohl
Institut für Angewandte Physik, Germany

Scanning Microscopy Supplement 4, 1990 (Pages 17-26)
Scanning Microscopy International, Chicago (AMF O'Hare), IL 60666 USA

0892-953X/90$3.00+.00

Spatially Sensitive Electron Energy Loss Spectroscopy

Helmut Kohl,
Institut für Angewandte Physik,
TH Darmstadt,
6100 Darmstadt, GERMANY

Abstract

Over the last decade electron energy loss spectroscopy has been increasingly used as a microanalytical technique. Under favorable conditions a spatial resolution better than 1 nm has been achieved. It is therefore possible to obtain spectroscopic information at an atomic scale. Such a spectrum can be used for the investigation of

- the elemental composition
- defect levels
- surface excitations
- the fine structure.

The spatial sensitivity of such experiments implies, that the initial or the final state of the scattered electrons must have a spatial structure. The theory for the scattering of wave packets will be discussed, focussing on the implications for the attainable spatial sensitivity in energy filtered images as well as in site-specific electron energy loss spectroscopy.

Key words: Electron energy loss spectroscopy, inelastic scattering cross section, inner shell ionisation, energy filtered imaging, spatial resolution, channeling, site specific spectroscopy.

Address for correspondence:
Helmut Kohl
Institut für Angewandte Physik
Technische Hochschule Darmstadt
Hochschulstraße 6
6100 Darmstadt, GERMANY

Tel.: (49)6151/162181
FAX: (49)6151/165489

Introduction

Scattering experiments yield a wealth of information about physical objects. For the investigation of solids x-rays, neutrons, ions or electrons are used as incident particles. One can distinguish between elastic and inelastic scattering processes. In the former case the object remains in its initial state, whereas in the latter case it undergoes a transition to an excited state. By elastic scattering experiments such as x-ray or neutron diffraction one therefore probes the initial state (most often the ground state) of the object. Inelastic scattering processes probe the energy levels of the specimen. We shall focus our interest on a particular technique, namely electron energy-loss spectroscopy. For a recent review of the technique see Egerton (1986).

More specifically, we shall deal with the excitation of core-levels by high-energy incident electrons in the transmission mode. From such a spectrum one can obtain different types of information. The signal under characteristic edges permits an analysis of the chemical composition of the specimen on a microscopic scale. Under favorable conditions a spatial resolution of less than 1 nm has been demonstrated (Ottensmeyer and Andrew, 1980; Scheinfein and Isaacson, 1986; Mory et al., 1988). The finer details of the spectrum yield information on the chemical state of a particular element in the specimen.

The Differential Cross-Section

We assume that high-energy electrons are transmitted through a thin specimen, so that only single scattering processes have to be considered. Then the first-order Born approximation can be used to calculate the differential cross section. The transition rate w from an initial state $|I\rangle$ to a final state $|F\rangle$ under a perturbation V is determined by Fermi's golden rule (Landau and Lifshitz, 1965):

$$w_{IF} = \frac{2\pi}{\hbar} \; |\langle F| V| I\rangle|^2 \; \delta(E_I - E_F) \; . \qquad (1)$$

In a scattering experiment the initial state is given by a product state of an incident plane wave with a

Table of Symbols

$A(\vec{\alpha})$	aperture function
a_H	Bohrs radius
α_o	objective aperture angle
β_o	spectrometer acceptance angle
C_s	spherical aberration constant
$C_{\vec{g}}^{(j)}$	Bloch wave coefficient
$\gamma(\vec{\alpha})$	phase shift due to lens aberrations
$D(\vec{\beta})$	detector function
d	thickness of the crystal
E_F	total energy of the final state
E_H	Rydbergs energy
E_I	total energy of the initial state
E_o	energy of the incident electrons
e_o	charge of the electron
ΔE	energy loss
$\varepsilon(\vec{K},\omega)$	dielectric funtion
$\frac{df(E,\vec{K})}{dE}$	generalized oszillator strength
$\|f\rangle$	final state of the object
$\|F\rangle$	final state of the total system
Δf	defocus
H_o	Hamilton operator of the object
$\hbar$	Plancks constant
$\|i\rangle$	initial state of the object
$\|I\rangle$	initial state of total system
I_o	current of the incident beam
$j_1(x)$	spherical Bessel function
$\vec{K},\vec{K}'$	scattering vectors
$\vec{k}^{(j)}$	wave vector of the j-th Bloch wave
k_B	Boltzmann constant
$\vec{k}_f$	wave vector of the scattered electron
$\|\vec{k}_f\rangle$	final state of the scattered electron
$\vec{k}_i$	wave vector of the incident electron
$\|\vec{k}_i\rangle$	initial state of the incident electron
$\varkappa$	wave number of the emitted electron
m	electron mass
$\Phi_{nlm}(\vec{r})$	atomic wave function
$R_{nl}(r)$	radial wave funtion
$\vec{r}_j$	position of the j-th electron in the object
$\vec{\rho}$	center of the spot
$(\vec{\rho}_o,z_o)$	coordinates in the object plane
$\rho(\vec{r})$	electron density
$\rho_{\vec{K}}$	Fourier transform of the electron density
$S(\vec{K},\omega)$	dynamic form factor
$S(\vec{K},\vec{K}',\omega)$	mixed dynamic form factor
$\frac{d^2\sigma}{d\Omega d(\Delta E)}$	double differential cross section
Θ_E	characteristic angle for inelastic scattering
V	interaction potential
w	transition rate
$Y_{lm}(\vartheta,\varphi)$	spherical harmonic

wave vector $\vec{k}_i$ and the initial state $|i\rangle$ of the object:

$$|I\rangle = |\vec{k}_i\rangle |i\rangle \quad . \tag{2}$$

Correspondingly the final state is given by:

$$|F\rangle = |\vec{k}_f\rangle |f\rangle \quad , \tag{3}$$

where $\vec{k}_f$ denotes the wave vector of the scattered electron and $|f\rangle$ the final state of the object.

Following the procedure of Bethe (1930) as outlined by Landau and Lifshitz (1965) we obtain for the differential cross section for the transition $i \rightarrow f$:

$$\frac{d\sigma_{if}}{d\Omega} = \frac{m^2}{4\pi^2\hbar^4}\frac{k_f}{k_i} \left| \langle f\, \vec{k}_f \right| V \left| i\, \vec{k}_i \right\rangle \Big|^2 . \tag{4}$$

Considering that the perturbation V is given by the Coulomb interaction between the incident electron and the electrons in the specimen, we obtain:

$$\frac{d\sigma}{d\Omega d(\Delta E)} = \frac{4k_f}{a_H^2\, k_i K^4} \sum_f \left| \langle f \left| \sum_j \exp(-i\vec{K}\vec{r}_j) \right| i \right\rangle \Big|^2 \delta(E_i - E_f - \Delta E) \tag{5}$$

where $\vec{K} = \vec{k}_i - \vec{k}_f$ is the scattering vector and $\vec{r}_j$ the position of the j-th electron in the object. As the final state is not determined, we have to sum over all final states corresponding to a given energy loss ΔE. The matrix element contains only object properties.

The Characterisation of Object Properties

Before we proceed to the actual computation of the cross section we shall discuss several quantities related to the square of the matrix element in eq. (5). Following Bethe (1930) one defines the generalized oscillator strength per unit energy (for continuum states)

$$\frac{df(E,\vec{K})}{dE} = \frac{2mE}{\hbar^2K^2}$$

$$\sum_f |< f | \sum_j \exp(-i\vec{K}\vec{r}_j)| i >|^2 \delta(E_i - E_f - E) \qquad (6)$$

This quantity has been discussed by Bonham (1990) and Bichsel (1990). In the limit $K \to 0$ it is equal to the optical oscillator strength.

From a thermodynamic point of view one is interested in correlation functions. We define an operator $\rho_{\vec{K}}$ to describe the Fourier transform of the electron density

$$\rho(\vec{r}) = \sum_j \delta(\vec{r} - \vec{r}_j) \qquad (7)$$

in the object. The Fourier-transform is given by:

$$\rho_{\vec{K}} = \int \rho(\vec{r}) \exp(-i\vec{K}\vec{r})\, d^3\vec{r} = \sum_j \exp(-i\vec{K}\vec{r}_j) \qquad (8)$$

Its time evolution in the Heisenberg representation can be formally written as:

$$\rho_{\vec{K}}(t) = \exp\left(\frac{i}{\hbar} H_o t\right) \rho_{\vec{K}} \exp\left(-\frac{i}{\hbar} H_o t\right) , \qquad (9)$$

where H_o denotes the Hamilton operator of the object. The Fourier transform (with respect to the time) of the density-density correlation function:

$$S(\vec{K}, \omega) = \frac{1}{2\pi} \int_{-\infty}^{\infty} < \rho_{\vec{K}}(t)\, \rho_{-\vec{K}} >_T \exp(i\omega t)\, dt \qquad (10)$$

is the so-called dynamic form factor (van Hove, 1954). The brackets $< >_T$ denote the thermal average. Evaluating eq. (10) using eigenstates of the Hamilton-operator H_o, we obtain (Kittel, 1964):

$$S(\vec{K}, \omega) = \frac{1}{2\pi} \sum_{i,f} P_i$$

$$\int_{-\infty}^{\infty} < i | \exp(\frac{i}{\hbar} H_o t)\, \rho_{\vec{K}} \exp(-\frac{i}{\hbar} H_o t) | f >$$

$$< f | \rho_{-\vec{K}} | i > e^{i\omega t}\, dt = \sum_{i,f} P_i | < i | \rho_{\vec{K}} | f > |^2$$

$$\times \frac{1}{2\pi} \int_{-\infty}^{\infty} \exp\left[i(\omega_i - \omega_f + \omega)\, t\right] dt$$

$$= \sum_{i,f} P_i | < i | \rho_{\vec{K}} | f > |^2 \delta(\omega_i - \omega_f + \omega) , \qquad (11)$$

where P_i is the probability that the object is initially in the state $|i>$. If the object is in its ground state, $S(\vec{K}, \omega)$ is equal to the sum over the final states in eq. (5) (apart from a factor $\hbar$).

Another related quantity is the dielectric function $\varepsilon(\vec{K}, \omega)$. Using the dissipation - fluctuation theorem it can be shown that (Platzman and Wolff, 1973):

$$S(\vec{K}, \omega) = - \frac{\varepsilon_o \hbar K^2 V}{\pi e_o^2 \left[1 - \exp(-\frac{\hbar\omega}{k_B T})\right]} \operatorname{Im} \frac{1}{\varepsilon(\vec{K}, \omega)} . \qquad (12)$$

This equivalence permits us to compute the dielectric function from experimental energy loss spectra measured in the forward direction ($\vec{K} \to \vec{0}$). This approach is extremely valuable for the determination of the dispersion and absorption of matter in the vacuum UV and soft x-ray range (Raether, 1980; also see Schattschneider, 1990).

The Matrix Element for Free Atoms

We shall now focus on inner-shell excitations. If one is interested in the chemical composition of the specimen, it is natural to approximate the total cross section by the sum of free-atom cross sections. We thereby neglect the fine structure in the energy loss spectrum. For microanalytical purposes one uses the signal in a rather large energy window, thus averaging over the finer details. It has been demonstrated by explicit calculations that the error introduced by the free-atom model is small (Weng and Rez, 1988) as compared to the overall accuracy of the current quantitation procedures (Hofer and Golob, 1988). Generally one uses the central-field model for quantitative calculations, thereby considering the electron-electron interaction only in a rather global manner. The merits and drawbacks of this approximation have been reviewed by Starace (1982). Using a central potential, the eigenfunctions can be written as (Manson, 1972):

$$\Phi_{nlm}(\vec{r}) = R_{nl}(r)\, Y_{lm}(\vartheta, \varphi) \qquad (13)$$

for the (bound) initial state with the quantum numbers n,l,m and

$$\Phi_{\varkappa l_1 m_1}(\vec{r}) = R_{\varkappa l_1}(r)\, Y_{l_1 m_1}(\vartheta, \varphi) \qquad (14)$$

for the final state, where the formerly bound electron leaves the atom with an energy $\hbar^2\varkappa^2/2m$. Using the expansion of a plane wave into spherical harmonics:

$$\exp(i\vec{K}\vec{r}) = \qquad (15)$$

$$4\pi \sum_{l_2, m_2} i^{l_2}\, j_{l_2}(Kr)\, Y^*_{l_2 m_2}(\vartheta_{\vec{K}}, \varphi_{\vec{K}})\, Y_{l_2 m_2}(\vartheta, \varphi)$$

we obtain for the matrix element

$$< \varkappa\, l_1\, m_1 \mid \exp(i \vec{K} \vec{r}) \mid n\, l\, m > =$$

$$\sum_{l_2, m_2} i^{l_2}\, Y^{*}_{l_2 m_2}\left(\vartheta_{\vec{K}}, \varphi_{\vec{K}}\right) (-1)^{m_1} \sqrt{(2l+1)\,(2l_1+1)} \times$$

$$\begin{pmatrix} l_1 & l_2 & l \\ 0 & 0 & 0 \end{pmatrix} \begin{pmatrix} l_1 & l_2 & l \\ -m_1 & m_2 & m \end{pmatrix} \times$$

$$\int R_{\varkappa l_1}(r)\, j_{l_2}(Kr)\, R_{nl}(r) r^2\, dr \qquad (16)$$

where

$$\begin{pmatrix} : & : & : \end{pmatrix}$$

denotes a 3-j symbol (Messiah, 1964). For a quantitative computation one has to determine the radial wave functions for a given potential and then the integral in eq. (16). In general these steps have to be performed numerically. Only for a hydrogenic model can the generalized oscillator strength be calculated analytically. This has been done by Egerton (1979, 1981, 1986) for the excitation of K and L electrons. Subsequent comparisons with experimental data taken on standards indicate, that the K-shell cross sections are accurate to within about 10%, whereas for L-shells larger deviations occur (Hofer and Golob, 1988). Extensive numerical calculations have been undertaken by Leapman et al. (1980), Rez (1982) and Ahn and Rez (1985).

The Scattering of Wave Packets

In the preceding chapters we have dealt with the scattering of an electron from one plane wave state into another. It is obvious that for such a situation the scattering probability will be independent of the position of the scatterer. To obtain any spatial information, we have to impose a spatial structure onto the incident (or the scattered) wave. To demonstrate the principle we consider the coherent superposition of two plane waves as depicted in Fig. 1. Such an initial state can be prepared by means of a biprism. On the specimen we find interference fringes. In other words, the intensity distribution is sinusoidally modulated. The initial state is a product state of the incident electron and the object. It is described by:

$$\frac{1}{\sqrt{2}}\left[\exp(i\vec{k}\vec{r}) + \exp(i\varphi)\exp(i\vec{k}'\vec{r})\right]|i> = \frac{1}{\sqrt{2}}\left[|\vec{k}\, i> + \exp(i\varphi)|\vec{k}'\, i>\right], \qquad (17)$$

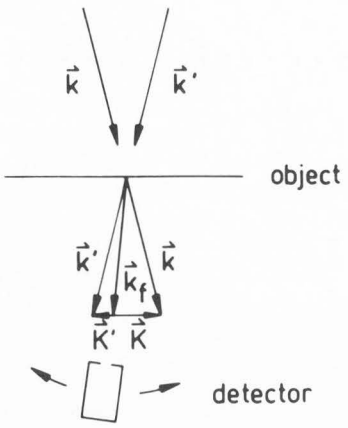

Fig. 1 Experimental arrangement to measure interference effects in elastic and inelastic scattering. The object is illuminated by a coherent superposition of plane waves with the wave vector $\vec{k}$ and $\vec{k}'$. The detector registers the intensity in the direction of $\vec{k}_f$.

where $| i >$ denotes the initial object state.

The phase factor $\exp(i\varphi)$ controls the position of the intensity maxima. To calculate the transition probability to the final state:

$$\exp(i \vec{k}_f \vec{r}) \mid f > = \mid \vec{k}_f f >$$

we use first order perturbation theory. The approximations are exactly equivalent to those used in the preceding chapters. To obtain the transition rate w, we have to sum over all possible final states with a given energy:

$$w = \frac{2\pi}{\hbar^2}\frac{1}{2} \times$$

$$\sum_f \left| < \vec{k}_f f \mid V\left(\mid \vec{k}\, i > + \exp(i\varphi) \mid \vec{k}'\, i > \right) \right|^2$$

$$\times\ \delta(\omega_i - \omega_f + \omega) =$$

$$= \frac{\pi}{\hbar^2} \sum_f \left(| < \vec{k}_f f \mid V \mid \vec{k}\, i > |^2 + \right.$$

$$+ | < \vec{k}_f f \mid V \mid \vec{k}'\, i > |^2 +$$

$$+ \exp(i\varphi) < \vec{k}\, i \mid V \mid \vec{k}_f f > < \vec{k}_f f \mid V \mid \vec{k}'\, i > +$$

$$\left. + \exp(-i\varphi) < \vec{k}'\, i \mid V \mid \vec{k}_f f > < \vec{k}_f f \mid V \mid \vec{k}\, i > \right)$$

$$\times\ \delta(\omega_i - \omega_f + \omega). \qquad (18)$$

This generalizes our eq. (1). It is interesting to note that the scattering of wave packets composed of a coherent superposition of plane waves has already been discussed in Born's (1926) pioneering paper on quantum mechanical scattering processes.

By algebraic manipulations, similar to those outlined in chapter 3, one can show that the spatial object properties are contained in the so-called "mixed dynamic form factor" (Rose, 1976; Kohl and Rose, 1985), which is defined as:

$$S(\vec{K}, \vec{K}', \omega) = \frac{1}{2\pi} \int_{-\infty}^{\infty} \langle \rho_{\vec{K}}(t)\, \rho_{-\vec{K}'} \rangle_T \exp(i\omega t)\, dt, \quad (19)$$

where $\vec{K}' = \vec{k}' - \vec{k}_f$ is the second scattering vector involved in our set-up. Again, this quantity can be related to a generalized dielectric function. We note that spatially homogeneous media (such as a free electron gas) are completely described by the function $S(\vec{K},\omega) = S(\vec{K},\vec{K},\omega)$ (Pines, 1964). For $\vec{K} \neq \vec{K}'$ the mixed dynamic form factor is nonzero only for inhomogeneous media (Kohl and Rose, 1985). The contributions where $\vec{K} \neq \vec{K}'$ therefore describe the spatial structure of the excitation.

The Theory of Image Formation

In a scanning transmission electron microscope (STEM) the electrons are focussed onto a small spot ($d \approx 5$ Å) on the specimen. This spot is scanned over the object. The count rate of the scattered electrons is displayed as grey level on a synchroneously deflected cathode ray tube.

The initial state of the electrons is now given by a coherent superposition of all plane waves passing the objective aperture

$$\exp(ik_o z_o) \times$$

$$\int A(\vec{\alpha}) \exp(-i\gamma_o(\vec{\alpha})) \exp(ik_o(\vec{\rho}_o - \vec{\rho})\vec{\alpha})\, d^2\vec{\alpha} \quad (20)$$

where $A(\vec{\alpha})$ denotes the aperture function. For a circular aperture subtending an angle α_o we find:

$$A(\vec{\alpha}) = \begin{cases} 1 & \text{for} \quad |\vec{\alpha}| < \alpha_o \\ 0 & \text{otherwise} \end{cases} \quad (21)$$

The phase shift,

$$\gamma_o(\vec{\alpha}) = k_o \left(\frac{C_s}{4} \alpha^4 - \frac{\Delta f}{2} \alpha^2 \right) \quad (22)$$

introduced by the objective lens depends both on the coefficient of the spherical aberration C_s and the defocus Δf. The vectors $\vec{\rho}_o$ and $\vec{\rho}$ denote the position of an object point and the position of the center of the spot, respectively. Using this expression and integrating over all angles $\beta < \beta_o$ subtended by the detector, we obtain for the current per unit energy in the detector (Rose, 1976; Kohl and Rose, 1985):

$$\frac{dI}{dE} = \frac{I_o}{\pi^3 \alpha_o^2 \hbar} \frac{k\, k_o^3 E_H}{E_o} \times$$

$$\int A(\vec{\alpha})\, A(\vec{\alpha}')\, D(\vec{\beta}) \exp(i\{\gamma_o(\vec{\alpha}) - \gamma_o(\vec{\alpha}')\}) \times \quad (23)$$

$$\exp(ik_o \vec{\rho}(\vec{\alpha} - \vec{\alpha}')) \frac{S(\vec{K},\vec{K}',\omega)}{K^2 K'^2} d^2\vec{\alpha}\, d^2\vec{\alpha}'\, d^2\vec{\beta},$$

where

$$D(\vec{\beta}) = \begin{cases} 1 & \text{for} \quad |\vec{\beta}| < \beta_o \\ 0 & \text{otherwise} \end{cases} \quad (24)$$

denotes the detector function, I_o the incident beam current, β_o the spectrometer acceptance angle (at the specimen), $E_H = 13{,}6$ eV is Rydberg's energy and E_o the energy of the incident electrons. The scattering vectors $\vec{K}$ and $\vec{K}'$ are given by:

$$\vec{K} = k_o \left[\Theta_E \vec{e}_z + (\vec{\alpha} - \vec{\beta}) \right]$$

and

$$\vec{K}' = k_o \left[\Theta_E \vec{e}_z + (\vec{\alpha}' - \vec{\beta}) \right],$$

where $k_o = 2\pi/\lambda$ is the wave number of the incident electrons and $\Theta_E = \Delta E/2E_o$ the characteristic angle for inelastic scattering with an energy loss ΔE.

In eq. (23) the integrations are performed over the reciprocal (angular) variables $\vec{\alpha}$ and $\vec{\alpha}'$. An alternative formulation in real space has been given by Ritchie and Howie (1988). As the equations are entirely equivalent it is a question of computational efficiency which one is used in a particular case.

Quantitative studies of "inelastic images" have been undertaken for plasmons and for inner-shell losses. The former subject is treated in detail by Ritchie (1990). Images using the surface plasmon loss electrons have been shown to permit a spatial resolution of a few nanometers (Batson, 1982 a, b, 1985; Achèche et al., 1986). This is in good agreement with theoretical predictions (Schmeits, 1981 ; Ritchie, 1981; Kohl, 1983, Ferrell and Echenique, 1985; Ritchie and Howie, 1988).

We shall now discuss the resolution attainable in elemental maps. So far, three different criteria have been used to determine the resolution. Scheinfein and Isaacson (1986) have measured the intensity distribution crossing a Si/CaF_2 interface. Within the experimental error, the Si-L_{23} loss signal ($\Delta E = 99$ eV) decays within 5Å from the interface.

Shuman et al. (1986) have taken images of an uranium-stained catalase crystal using the U - O_{45} loss at $\Delta E = 112$ eV. Taking the Fourier-transform of their images, they obtained the transfer function at spatial frequencies corresponding to reciprocal lattice vectors. As they used a conventional transmission electron microscope, the transfer of the higher spatial frequencies was greatly damped due to

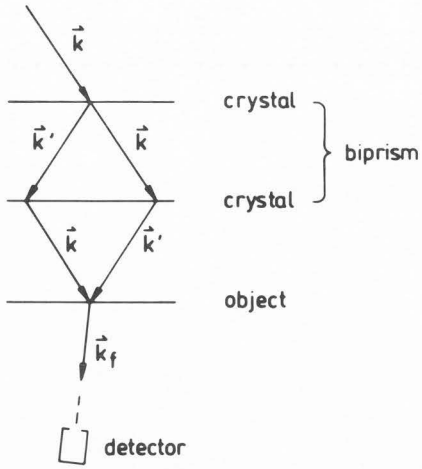

Fig. 2 Set-up to create lattice periodic wave fields. The two upper crystal plates constitute a biprism, the lower crystal is the specimen.

the axial chromatic aberration of the objective lens. Their method is very promising. One has to take care, however, that the crystal is thin enough so that multiple elastic-inelastic processes are unlikely to occur.

Mory et al. (1988) have imaged a random distribution of small urani m clusters using the U-O_{45} loss. The half width ' the peak of the cross-correlation function between two simultaneously taken pictures constitutes a good measure of the resolution in the image. This method has been extensively used by Frank (1980) for phase-contrast images. In a STEM it is possible to obtain a dark-field signal simultaneously with the inelastic image. Mory et al. (1988) have used the former to characterize the cluster sizes and compared the resolution (judged by the cross-correlation method) of the dark-field images with the resolution in the U-O_{45} loss images. In the inelastic image the resolution was only slightly worse than in the elastic one. The best resolution determined in a U-O_{45} loss image was 4.2 Å (Mory, personal communication).

These experiments clearly demonstrate that sub-nanometer resolution can be obtained with images taken at an energy loss of about 100 eV. This is in good agreement with calculations using the dipole approximation for the scattering matrix element (Kohl and Rose, 1985).

Site Specific Electron Energy Loss Spectroscopy

A method to build a biprism for electrons is to use crystal plates as schematically shown in Fig. 2 (Marton, 1952), oriented so that a Bragg-reflex is excited. The first two crystal plates constitute a biprism, the third one corresponds to the specimen. As there are no optical elements in this setup, it can be used equally well for x-ray and neutron interferometry (Bonse and Hart, 1965 ; Rauch et al. 1974). The distance between the crystal plates is determined by the requirements of the interferometric experiment. When diminishing the distance to zero we have one oriented crystal left. In it the wave field is modulated with a period corresponding to the excited reciprocal lattice vector. In particle physics this is named the "channeling effect". The position of the maxima can be varied by slightly tilting the crystal. The scattering probability will then depend on the exact orientation of the specimen. Correspondingly, the emitted secondary radiation (x-rays, Auger-electrons etc.) will be orientation dependent. This effect is used in the ALCHEMI (Atomic Location by Channeling Enhanced Microanalysis) technique proposed by Taftø (1982) and discussed by Krishnan (1989) at this conference.

The variation of the double differential cross-section near the iron L_{23} edge has been used by Taftø and Krivanek (1982) to determine the valency of Fe-ions on different sites in a chromite crystal. Taftø (1984) has investigated the fine structure of the Al K-edge in sillimanite. In this crystal there are octahedrally as well as tetrahedrally coordinated Al-atoms, which have different fine structures. By varying the orientation of the crystal he could determine the origin of characteristic structures in the spectrum. Thus it is possible to obtain energy loss spectra which stem predominantly from one site. The practical application was hindered by the rather low signal level. The recent advent of parallel recording spectrometers should help to circumvent these limitations.

The practical application of site specific electron energy energy loss spectroscopy necessitates prior knowledge of the scattering probabilities from the different sites as a function of crystal orientation. We shall now briefly review recent theoretical advances in this field.

The important point is that the initial and final state of the incident electron is given by a coherent superposition of Bloch waves. In the following we shall assume that the crystal is thin enough, so that only single inelastic scattering processes occur. The multiple elastic scattering is taken into account by use of the Bloch-wave formalism. Following Maslen (1987) we shall therefore use first-order perturbation theory for the inelastic scattering processes between Bloch waves. This method is equivalent to the distorted wave Born approximation, which is frequently used in nuclear physics. The initial state of the incident electron is given by (Metherell, 1975):

$$\psi_i(\vec{r}) = \sum_{\vec{g},j} C_o^{(j)*} C_{\vec{g}}^{(j)} \exp\left[i(\vec{k}^{(j)} + \vec{g})\,\vec{r} \right] . \qquad (25)$$

Outside the crystal, the scattered electron is described by a plane wave with wave vector $\vec{k}'$. Taking into account the boundary conditions at the exit surface, we obtain for the wave function after the scattering (Maslen and Rossouw, 1984; Saldin and

Rez, 1987; Weickenmeier, 1987):

$$\psi_f^{|}(r) = \sum_{i^{|},\vec{h}^{|}} C_o^{(i^{|})*}\, C_{\vec{h}^{|}}^{(i^{|})} \exp\left[+ i\left(k_z - k_z^{(i^{|})}\right) d\right] \times$$

$$\exp\left[i\left(\vec{k}^{(i^{|})} + \vec{h}^{|}\right)\vec{r}\right] \quad , \qquad (26)$$

where d denotes the thickness of the crystal.

For the calculation of the transition matrix element, the functions (25) and (26) have to be multiplied by the wave function of the initial and the final object state, respectively. For these we shall use atomic wave functions. The transition matrix element for an atom at a position $\vec{R}_a$ is then given by:

$$< F \mid V \mid I > =$$

$$\sum_{j,\,\vec{g}\,,\,i^{|}\,,\,\vec{h}^{|}} C_o^{(j)*}\, C_{\vec{g}}^{(j)}\, C_o^{(i^{|})}\, C_{\vec{h}^{|}}^{(i^{|})*}$$

$$\times \exp\left[-i\left(k_z - k_z^{(i^{|})}\right) d\right] \quad W_{if}(\vec{Q}_1)\, \frac{\exp\left[i\,\vec{Q}_1\,\vec{R}_a\right]}{\varepsilon_o\, Q_1^2} \quad , \qquad (27)$$

where

$$W_{if}(\vec{Q}_1) = < f \mid \exp(i\vec{Q}_1\vec{r}) \mid i > =$$

$$\int \varphi_f^*(\vec{r})\ \varphi_i(\vec{r}) \exp(i\vec{Q}_1\vec{r})\, d^3\vec{r}$$

and

$$\vec{Q}_1 = \vec{k}^{(j)} - \vec{k}^{(i^{|})} + \vec{g} - \vec{h}^{|}$$

To compute the cross-section, we have to take the modulus square and sum over all final states with an energy $E_f = E_i + \Delta E$. This includes a sum over all positions $\vec{R}_a$ of the atomic species considered. We obtain (Maslen and Rossouw, 1984; Maslen, 1987; Saldin and Rez, 1987)

$$\sum_{f,\vec{R}_a} \sum_{\substack{j,\vec{g},i^{|},\vec{h}^{|} \\ j^{|},\vec{g}^{|},i,\vec{h}}} C_o^{(j)*}\, C_{\vec{g}}^{(j)}\, C_o^{(i^{|})}\, C_{\vec{h}^{|}}^{(i^{|})*}$$

$$\times \quad C_o^{(j^{|})}\, C_{\vec{g}^{|}}^{(j^{|})*}\, C_o^{(i)*}\, C_{\vec{h}}^{(i)}$$

$$\times \quad \frac{\exp[i(\vec{Q}_1 - \vec{Q}_2)\,\vec{R}_a]}{\varepsilon_o^2\, Q_1^2\, Q_2^2} \exp\left[i(k_z^{(i^{|})} - k_z^{(i)})\, d\right]$$

$$\times \quad W_{if}(\vec{Q}_1)\, W_{if}^*(\vec{Q}_2) \quad \delta(E_i - E_f + \Delta E) \quad , \qquad (28)$$

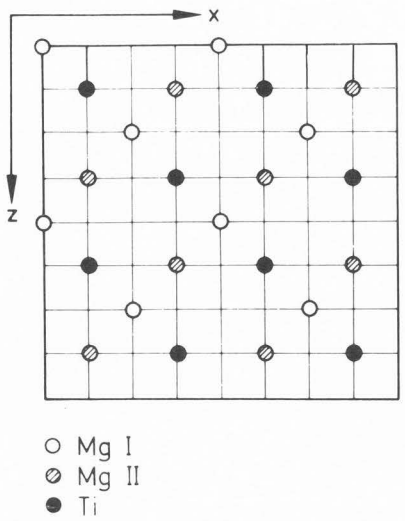

Fig. 3 Projection of the Mg_2TiO_4 unit cell onto the x-z plane. For simplicity we have omitted the oxygen atoms. The lattice constant is equal to a = 8.441Å. (From Weickenmeier and Kohl (1989). Copyright 1989 Taylor & Francis Ltd., London).

where

$$\vec{Q}_2 = \vec{k}^{(i)} - \vec{k}^{(j^{|})} + \vec{h} - \vec{g}^{|}$$

The calculation of the matrix elements $W_{if}(\vec{Q})$ has been discussed in chapter 3. For numerical evaluations two alternative routes have been taken. Maslen and Rossouw (1984) and Saldin and Rez (1987) have performed the summations over $\vec{R}_a$ analytically. Then the time requirements are set by the N^8 terms in the sum over the Bloch-wave coefficients.

Alternatively Weickenmeier and Kohl (1989) have rewritten eq. (28) as a sum over squares of expression like (27). In this case the number of Bloch-wave terms is proportional to N^4. The summation over $\vec{R}_a$ however, has then to be performed numerically. To demonstrate the feasibility of such calculations we quote a result on Mg_2TiO_4 . The projection of the structure onto the x-z plane is shown schematically in Fig.3 . We note, that there are two inequivalent types of planes.

For the calculations we have assumed a crystal oriented so that a (400) systematic row is excited. We have performed a 21-beam calculation for the differential cross-section in the forward direction for the K-excitation of Mg and Ti as a function of the crystal tilt (Weickenmeier and Kohl, 1989). The result is shown in Fig. 4. We observe, that for tilt-angles smaller than Θ_{400} the contribution of the Mg-II planes predominates, whereas for $\Theta > \Theta_{400}$ the scattering of the Mg-I planes is dominant. Thus it should be possible in the near future to interpret experimental results quantitatively.

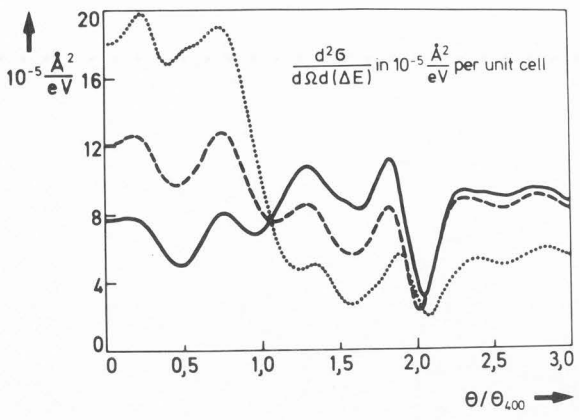

Fig. 4 Variation of the differential cross section in the forward direction as a function of the tilt angle Θ. We have assumed a 51 nm thick $Mg_2Ti\,O_4$ crystal, an incident energy E_o = 100 keV, and an energy loss of ΔE = 1405 eV for Mg and of ΔE = 5066 eV for Ti. (From Weickenmeier and Kohl (1989). Copyright 1989 Taylor & Francis Ltd., London).

Conclusion

To obtain a spatially sensitive signal it is necessary to impose a spatial structure unto the incident and/or the scattered electron. This can be done either by means of external electric and/or magnetic fields (namely electron lenses) or by the object itself. It has been recently demonstrated both experimentally and theoretically that sub-nanometer resolution is possible when imaging with energy-losses in the 100 eV range. Thus high-resolution elemental mapping is feasible, provided that the specimen is sufficiently radiation resistent.

Illumination of an oriented crystal by a parallel beam of electrons results in a Bloch-wave field within the crystal. If we measure the variation of the cross-section as a function of the tilt, we obtain a signal, which depends on the site of the scatterer within the unit cell. The feasibility of such site-specific EELS has been demonstrated by Taftø and Krivanek (1982). They could distinguish between the positions of Fe^{2+} and Fe^{3+} in a chromite spinell. Taftø (1984) has obtained spectra for Al in octahedral and tetrahedral sites. This method is very promising for the investigation of the local electronic structure in materials with a complicated unit cell.

Acknowledgements

I would like to acknowledge the stimulating cooperation with the STEM group at the Laboratoire de Physique des Solides in Orsay. In particular I wish to express my gratitude to Drs. C. Mory, C. Colliex and M. Tencé, who have performed the resolution tests. The results on site-specific spectroscopy have emerged from an enjoyable collaboration with my colleagues A. Weickenmeier and Dr. D. von Hugo at the TH Darmstadt. Thanks are also due to Professor H. Rose for valuable discussions.

References

Achèche M, Colliex C, Kohl H, Nourtier A, and Trebbia P. (1986) Theoretical and experimental study of plasmon excitations in small metallic spheres, Ultramicroscopy 20, 99-105.

Ahn CC, Rez P. (1985). Inner shell edge profiles in electron energy loss spectroscopy, Ultramicroscopy 17, 105-116.

Batson PE. (1982 a). A new surface plasmon resonance in clusters of small aluminium spheres, Ultramicroscopy 9, 277-282.

Batson PE. (1982 b). Surface Plasmon Coupling in Clusters of Small Spheres, Phys. Rev. Lett. 49, 936-940.

Batson PE. (1985). Inelastic Scattering of Fast Electrons in Clusters of Small Spheres, Surf. Science 156, 720-734.

Bethe H. (1930). Zur Theorie des Durchgangs schneller Korpuskularstrahlen durch Materie, Ann. Phys. 5, 325-400.

Bichsel H. (1990). Energy Loss of Electrons Below 10keV, Scanning Microscopy Supplement 4, 147-156.

Bonham RA. (1990) Scattering from Atoms and Molecules in the Free State by Electrons with Energies Below 10 keV, Scanning Microscopy Supplement 4, 1-15.

Bonse H, Hart M. (1965). An X-ray Interferometer, Appl. Phys. Lett. 6, 155-156.

Born M. (1926). Quantenmechanik der Stoßvorgänge, Zeitschr. Physik 38, 803-827.

Egerton, RF. (1979) K-shell ionization cross-sections for use in microanalysis, Ultramicroscopy 4, 169-179.

Egerton, RF. (1981) SIGMAL: A program for calculating L-shell ionization cross-sections, Proc. 39th EMSA, (Claitor, Baton Rouge, LA) 198-199.

Egerton RF. (1986). Electron Energy Loss Spectroscopy (Plenum, New York), 1-410.

Ferrell TL, Echenique PM. (1985). Generation of Surface Excitations on Dielectric Spheres by an External Electron Beam, Phys. Rev. Lett. 55, 1526-1529.

Frank J. (1980). The role of correlation techniques in computer image processing. In: Computer Processing of Electron Microscope Images, P.W. Hawkes (ed.) (Springer, Berlin) pp. 187-222.

Hofer F, Golob P. (1988). Quantification of Electron Energy-Loss Spectra with K and L-Shell Ionization Cross-Sections, Micron and Microsc. Acta 19, 73-86.

Kittel C. (1964). Quantum Theory of Solids (Wiley, New York), 1-425.

Kohl H. (1983). Image formation by inelastically scattered electrons: Image of a surface plasmon, Ultramicroscopy 11, 53-65.

Kohl H, Rose H. (1985). Theory of image formation by inelastically scattered electrons in the electron microscope, Adv. Electr.& Electron Physics 65, 173-227.

Krishnan K. (1989). Channeling and Related Effects in Electron Microscopy: The Current Status, Scanning Microscopy Supplement 4, 157-170.

Landau LD, Lifshitz EM. (1965). Quantum Mechanics (Pergamon, Oxford), 571-580.

Leapman RD., Rez P, and Mayers DF. (1980). K, L, and M-shell generalized oscillator strengths and ionization cross sections for fast electron collisions, J. Chem. Phys. 72, 1232-1243.

Manson ST. (1972). Inelastic collisions of fast charged particles with atoms: ionization of the aluminium L Shell, Phys. Rev. A 6, 1013-1024.

Marton L. (1952). Electron interferometer, Phys. Rev. 85, 1057-1058.

Maslen V. (1987). On the role of inner-shell ionization in the scattering of fast electrons by crystals, Phil. Mag. B 55, 491-496.

Maslen V, Rossouw CJ. (1984). Implications of (e,2e) scattering for inelastic electron diffraction in crystals I. Theoretical, Phil. Mag. A 49, 735-742.

Messiah A. (1964). Quantum Mechanics, Vol. I (North Holland, Amsterdam), 1053-1060.

Metherell AF. (1975). Diffraction of electrons by perfect crystals. Electron Microscopy in Material Science, Vol. 2, 397-552.

Mory C, Bonnet N, Colliex C, Kohl H and Tencè M. (1988). Evaluation and Optimization of the Performance of Elastic and Inelastic Scanning Transmission Electron Microscope Imaging by Correlation Analysis, Scanning Microscopy, Supplement 2, 329-342.

Ottensmeyer FP, Andrew JW. (1980). High-Resolution Microanalysis of Biological Specimens by Electron Energy Loss Spectroscopy and by Electron Spectroscopic Imaging, J. Ultrastruc. Res. 72, 336-348.

Pines D. (1964). Elementary Excitations in Solids (Benjamin, New York), 1-299.

Platzmann PM, Wolff PA. (1973). Solid State Physics Suppl. 13, Waves and Interactions in Solid State Plasmas. (Academic, New York), 1-304.

Raether H. (1980). Excitation of Plasmons and Interband Transitions by Electrons, Springer Tracts in Modern Physics 88, 1-196.

Rauch H, Treimer W, and Bonse U. (1974). Test of a single crystal neutron interferometer, Phys. Lett. 47A, 369-371.

Rez P. (1982). Cross -sections for energy loss spectrometry, Ultramicroscopy 9, 283-288.

Ritchie RH. (1981). Quantal aspects of the spatial resolution of energy-loss measurements in electron microscopy I. Broad-beam geometry, Phil. Mag. A 44, 931-942.

Ritchie RH. (1990). Plasmons in Electron Spectra, Scanning Microscopy Supplement 4, 45-56.

Ritchie RH, Howie A. (1988). Inelastic scattering probabilities in scanning transmission electron microscopy, Phil. Mag. A 58, 753-767.

Rose H. (1976). Image formation by inelastically scattered electrons in electron microscopy, Optik 45, 139-158 and 187-208.

Saldin D, Rez P. (1987). The theory of the excitation of atomic inner-shells in crystals by fast electrons, Phil. Mag. B 55, 481-489.

Schattschneider P. (1990). Interband Transitions and Compton Scattering in EELS, Scanning Microscopy Supplement 4, 37-34, 35-43.

Scheinfein M , Isaacson MS. (1986). Electronic and chemical analysis of flouride interfacial structures at subnanometer spatial resolution, J. Vac. Sci. Technol. B 4 , 326-332.

Schmeits M. (1981). Inelastic Scattering of fast electrons by spherical surfaces, J. Phys. C 14, 1203-1216.

Shuman H, Chang CF, and Somlyo AP. (1986). Elemental imaging and resolution in energy-filtered conventional electron microscopy, Ultramicroscopy 19, 121-133.

Starace A. (1982). Theory of Atomic Photoionization, in: Handbuch der Physik, Band 31 (Springer, Berlin) pp. 1-121.

Taftø J. (1982). The cation-atom distribution in a (Cr, Fe, Al, $Mg)_3O_4$ spinel as revealed from the channeling effect in electron-induced X-ray emission, J. Appl. Cryst. 15, 378-381.

Taftø, J. (1984). Absorption Edge Fine Structure Study with Subunit Cell Spatial Resolution Using Electron Channeling, Nucl. Instr. and Methods B2, 733-736.

Taftø J, O. L. Krivanek (1982). Site-Specific Valence Determination by Electron Energy Loss Spectroscopy, Phys. Rev. Lett. 48, 560-563.

van Hove L. (1954). Correlations in Space and Time and Born Approximation Scattering in Systems of Interacting Particles, Phys. Rev. 95, 249-263.

Weickenmeier A. (1987). Berechnung des differentiellen Wirkungsquerschnitts für die Anregung innerer Schalen durch schnelle Elektronen in Kristallen. Diplom-Thesis, TH Darmstadt.

Weickenmeier A, Kohl H. (1989). Computation of the atomic inner-shell excitation cross-sections for fast electrons in crystals, Phil. Mag., B 60, 467-479.

Weng X, Rez P. (1988). Solid state effects on core electron cross-sections used in microanalysis, Ultramicroscopy 25, 345-348.

Discussion with Reviewers

Peter Schultz: You suggest that spatial resolution limits are in part due to inner-shell excitations induced by large impact parameters. This contribution can be calculated by the EM impulse (virtual photon exchange) of the incident electron, and compared with the integrated effect of close collisions using the Møller (e - e) cross-section. Our calculations indicate that distant collisions can be important for K-shell ionization, but insignificant for L-shell (or greater). This means that distant collisions are probably not contributing to resolution broadening.

Author: The relative contributions of close and distant collisions depend strongly on the detailed experimental conditions. Important parameters are the characteristic angle $\Theta_E = \Delta E/2E_o$, and the angles α_o and β_o , which are typically about 10^{-2} in an electron microscope. Under these conditions the dipole approximation can be used. Then a degradation of the resolution occurs only for Θ_E below about 10^{-3} . For Θ_E much larger than about 10^{-2} , the minimum momentum transfer becomes so large, that the dipole approximation is no longer valid. Presumably you are thinking of a situation in that regime.

P. Schattschneider: The angular halfwidth $\Theta_{1/2}$ of any form factor (dynamic or static) qualitatively determines the spatial range d over which an incoming plane wave interacts with the scatterer by $d \approx \lambda/\Theta_{1/2}$. Why, then, is the criterion not valid in your example?
Author: The rule of thumb $d \approx \lambda/\Theta_{1/2}$ relies on the Heisenberg uncertainty principle, relating the standard deviations of position and momentum by:

$$\sqrt{\Delta x^2}\ \sqrt{\Delta p^2} \geq \frac{\hbar}{2} \quad .$$

Putting $d \approx \sqrt{\Delta x^2}$ and $\sqrt{\Delta p^2} \approx \hbar k_o \sqrt{\Delta\Theta^2}$ we obtain

$$d \geq \frac{1}{2k_o\sqrt{\Delta\Theta^2}} = \frac{\lambda}{4\pi\sqrt{\Delta\Theta^2}} \ ,$$

where $\Delta\Theta^2$ is the standard angular deviation. For the image calculations we have used the dipole approximation. In that case the angular distribution is a Lorentzian and the standard deviation diverges.

It should be noted that the standard deviation rather than the half-width is needed for that type of calculation.

C. Colliex: Borns (1926) paper is not easy to find. Can you develop on this point?
Author: In § 5 of his paper Born (1926) writes down the differential equation for the movement of a free particle

$$\Delta\psi + k^2 \psi = 0 \qquad (7)$$

and writes a little further down : " Die allgemeinste Lösung von (7) ist

$$\psi(\vec{r}) = u_o(\vec{r}) = \int c(\vec{s})\ e^{ik(\vec{r}\,\vec{s})} d\vec{\omega} \ , \ \ldots \qquad (11)$$

wo $\vec{s}$ ein Einheitsvektor und $d\vec{\omega}$ das Element des Raumwinkels ist. Sie stellt Trägheitsbewegungen aller möglichen Richtungen mit derselben Energie dar; nach unseren Prinzipien ist $|c(\vec{s})|^2$ die pro Raumwinkeleinheit gerechnete Anzahl der Teilchen, die in der Richtung $\vec{s}$ fliegen."
Translated into English, he says: "The most general solution of (7) is

$$\psi(\vec{r}) = u_o(\vec{r}) = \int c(\vec{s})\ e^{ik(\vec{r}\,\vec{s})} d\vec{\omega} \ , \qquad (11)$$

where $\vec{s}$ is a unit vector and $d\vec{\omega}$ the element of the solid angle. This solution represents the free movement in all possible directions with a given energy; following our principles $|c(\vec{s})|^2$ is the number of particles per unit solid angle flying in the direction of $\vec{s}$."

As we have used the small angle approximation, the correspondance is given by

$s_x = \alpha_x$, $s_y = \alpha_y$, $s_z \approx 1$ and

$$c(-\vec{s}) = A(\vec{\alpha})\ e^{-i\gamma(\vec{\alpha})}\ e^{-ik\vec{\rho}\vec{\alpha}}$$

leading directly to our equation (20).

C. Colliex: How do you drop the $ik_o \vec{\rho}_o(\vec{\alpha}' - \vec{\alpha})$ between eqs. (20) and (23)?
Author:
The expression in eq. (20) is the wave function in a STEM near the object plane

$$\psi_{\vec{\rho}}(\vec{r}_o) = \exp(ik_o z_o)$$

$$\int A(\vec{\alpha})\ \exp[-i\gamma_o(\vec{\alpha})]\ \exp[ik_o(\vec{\rho}_o - \vec{\rho})\vec{\alpha}]\ d^2\vec{\alpha}$$

Here $\vec{r}_o = (\vec{\rho}_o, z_o)$ is the variable, whereas $\vec{\rho}$ is a parameter defining the position of the spot. This parameter $\vec{\rho}$ is varied by use of the deflection coils. When calculating a matrix element, one has to integrate over the variable $\vec{r}_o$. As a simple case let us consider the calculation of a matrix element for the elastic scattering off a given potential $V(\vec{r}_o)$ from $\vec{k}_i$ to $\vec{k}_f$

$$\langle \vec{k}_f\ |V|\ \vec{k}_i \rangle = \int \exp(-i\vec{k}_f \vec{r}_o)\ V(\vec{r}_o)\ \exp(i\vec{k}_i \vec{r}_o) d^3\vec{r}_o = V(\vec{K}),$$

where $V(\vec{K})$ denotes the Fourier transform of the potential and $\vec{K} = \vec{k}_i - \vec{k}_f$.

In a STEM the initial state is given by the wave packet $\psi_{\vec{\rho}}(\vec{r}_o)$ rather than by a plane wave $\exp(i\vec{k}_i\vec{r}_o)$. The matrix element is then given by

$$\int \exp(-i\vec{k}_f\vec{r}_o)\ V(\vec{r}_o)\ \exp(i\ k_o(\vec{\rho}_o - \vec{\rho})\vec{\alpha})\ \exp(ik_o z_o)\ A(\vec{\alpha})$$

$$\times \exp\ [-\ i\ \gamma\ (\vec{\alpha})]\ d^3\vec{r}_o\ d^2\vec{\alpha} =$$

$$\int V[k_o(\vec{\alpha} - \vec{\beta})]\ A(\vec{\alpha})\ \exp\ [-i\gamma(\vec{\alpha})]\ \exp(-i\ k_o\ \vec{\rho}\ \vec{\alpha})\ d^2\vec{\alpha} \ ,$$

where $\vec{\beta}$ is a vector perpendicular to the optic axis defined by $\vec{k}_f = k_o \vec{e}_z + k_o\vec{\beta}$.

Thus the variables $\vec{\rho}_o$, z_o disappear by integration, whereas the parameter $\vec{\rho}$ remains, describing the spatial dependance of the signal.

The derivation for the inelastic case is outlined in Kohl and Rose (1985).